Development and validation of a driving simulator for traffic control using field data

Trinh Dinh Toan[a*], Soi Hoi Lam[b], Yiik Diew Wong[c], Meng Meng[d]

[a] *Department of Transportation Engineering, Thuyloi University, 175 Tay Son, Dong Da, Hanoi, Viet Nam*
[b] *Department of Civil and Environmental Engineering, University of Macau, Avenida da Universidade, Taipa, Macau, China*
[c] *School of Civil and Environmental Engineering, Nanyang Technological University Singapore, 50 Nanyang Avenue, Singapore 639798, Singapore*
[d] *School of Management, University of Bath, Bath, BA2 7AY, UK*
[*] *Corresponding author, Email: Trinhdinhtoan@tlu.edu.vn*

Abstract. This paper presents the development and validation of a driving simulator for ramp traffic control on expressways using a traffic simulator and control (TSC). The TSC consists of two main components: car-following model (CFM), and traffic controller (TC). The CFM simulates the car-following behavior and delivers aggregated traffic parameters to the TC to derive control actions. The CFM and TC are harmonized and integrated in a close-loop control manner, where the effects of the control by the TC are fed-back as inputs for the CFM in real-time applications. Although the car-following behavior of individual vehicles is simulated, the aggregated outputs such as average speed and flow rate from the model are the parameters of interest. For simplicity in the model development and validation and to capture lane-changing effects, the traffic in the multi-lane expressway where the data were obtained was equivalently represented as a single-lane system. The validation of the CFM was performed at a macroscopic level where aggregated outputs from the model were compared to observed data in a segment of the Pan Island Expressway of Singapore under various traffic conditions. The result shows that the simulated speed is not significantly different from the actual speed at 5% significance level, and the aggregated flow rate discrepancies fall in a small range, from 2.21% to 3.15%. This shows that the TSC model is a reliable model for traffic simulation and control applications.

Keywords: traffic simulator; microscopic simulation; car-following model; traffic control; model validation

1. Introduction

Simulation modeling has recently become a popular and successful method for studying and solving real-world problems as advanced computer technologies [1-5]. Traffic simulation models are useful tools in the study of traffic systems and in evaluation of traffic management and control strategies because they enable detailed analyses of traffic dynamics, and geometric conditions can be effectively controlled [2,6,7,8]. Traffic simulation models can be categorized into microscopic, mesoscopic, and macroscopic models [9]. Microscopic models examine the details of traffic stream and interactions between individual vehicles, whereas macroscopic models describe traffic flow from a global perspective using aggregated traffic variables, and the mesoscopic models possess features of both types of models [3,10,11,12]. It has been commonly acknowledged that macroscopic traffic variables always have their microscopic elements. Specifically, the key microscopic traffic variables are speed, spacing, and headway between individual vehicles, while the key corresponding macroscopic variables are average speed, density and flow rate of traffic stream. In macroscopic representation, speed is the average speed of individual vehicles, density is calculated as inversion of the average spacing, and flow rate is calculated as inversion of the average headway.

The key building block of microscopic traffic simulation models is the car-following model (CFM) [1,13,14,15]. CFM characterizes the longitudinal motion of vehicles using mathematical description of the behavior by which drivers follow the preceding vehicle in a traffic stream [16,17,18,19]. CFMs are typically modelled as a closed-loop control system, where the vehicle acceleration is the control variable, the speed differential between the lead and

follower vehicle is the stimulus, and the driver sensitivity fluctuates as a function of the speed and spacing between the lead and the following vehicles [20].

CFMs are classified into three types in [16,21]: stimulus-based models, safety-distance models, and action-point models. In stimulus-based models, the driver's reaction to the speed and position differences with the preceding vehicle governs the acceleration of a following vehicle (the General Motors models [21,22]). Safety-distance models [23] are based on the viewpoint that a following vehicle maintains a speed and distance so that it can stop safely in occurrence of a sudden brake of the preceding vehicle. Action-point models [24,25] suggest that a driver's driving behavior varies depending on the traffic state such as the free-flow or congested conditions. Alternatively, in [16,17,18,20,26] CFMs are classified into five groups: Gazis-Herman-Rothery (GHR) model, Collision Avoidance (CA) model, Linear Model, Fuzzy-logic-based model, and Optimal Velocity (OV) model. GHR model, which is an extended version of General Motors' model [9,27], serves as a foundation for other CFMs and is one of the most well-studied models [9,18,20,27,28,29]. We have carried out a thorough study on various types of CFM, including stimulus-based models, safety-distance models, and action-point models before working in detail with GHR model. According to the GHR model, the following vehicle's acceleration is proportional to the follower's speed, the difference in speed between the follower and the leader, and the space headway [27].

To develop successfully a simulation model, the credibility of the model is essential, and testing procedures must be established to realize the performance and reliability of the model [4,30]. The credibility of the model should be enhanced via calibration, while the performance of the calibrated model should be evaluated through validation [31]. Calibration is the process of fine-tuning model parameters to increase the model's capability to reflect local driver behavior and traffic characteristics [2,4,6,12,32]. Validation, on the other hand, is the process of checking whether a simulation model reasonably represents the real system for its intended use [6,31,33]. Validating a simulation model entails a set of measures of effectiveness (MOEs) that reflect model performance [2,4,30,33]. In the development and application of a microscopic traffic simulation model, validation is most important [33,34].

Ni et al. (2004) [4] classified validation techniques into qualitative and quantitative approaches. Qualitative approach, known also as subjective or informal techniques, entails visual comparison of the simulated and observed data using graphical displays. Quantitative approach, known also as objective or formal techniques, quantifies the difference between the simulated and the observed values using statistical quantities such as mean error (ME), mean absolute error (MAE), mean squared error (MSE) and root-mean-square error (RMSE). Various statistical techniques that have been used for quantifying the deviation of the simulated models from the real systems following the quantitative approach include goodness-of-fit measures, confidence intervals, and statistical tests [6,31,35,36].

Regardless of the validation techniques, it can be identified from the literature review that, by studying the statistical properties of the microscopic simulation, the models attempt to explain the behavior of macroscopic systems of the larger scale. To obtain macroscopic traffic metrics, traffic micro-simulation models are often used for the study. Specifically, the microscopic traffic simulation models usually require the description of fundamental relationship between macroscopic variables (speed, flow, and density) [30,34,37,38,39]. For example, in Benekohal (1991) [31] and Benekohal and Treiterer (1988) [40], the validation of CARSIM simulation model was performed at both microscopic and macroscopic levels. At the microscopic level, the speed change patterns and trajectories from CARSIM were compared with the observed trajectories. At the macroscopic level, the average speed, volume and density provided by CARSIM were compared with the aggregated field data.

There are large number of commercial microscopic traffic simulation packages such as CORSIM, MITSIM, AIMSUN2, VISSIM, PARAMICS, AUTOBAHN, INTEGRATION, etc. for various applications [34,41]. The models are generally well recognized with friendly user interface, comprehensive visualization and detailed statistical outputs [11,17]. However, the models are essentially stand-alone software packages that are not designed to integrate with other applications in a feedback control manner for real-time applications [11]. Despite the widespread use of traffic simulation models, research works on model validation are relatively scare [4,6,30]. While the validation methods and techniques are not new, little is known on using field data to validate a microscopic simulation model at the macroscopic level following a quantitative approach [42].

This research constitutes part of a broader research project [43] that develops a multi-stage fuzzy logic controller (MS-FLC) for ramp traffic control on expressways. In the MS-FLC, the 3rd stage involves formulation and implementation of actions for ramp control using fuzzy-logic control algorithm. For these tasks, a traffic simulator and control (TSC) that consists of a driving simulator, named in this paper as the car-following model (CFM), and a traffic controller (TC) were developed. Given that the model development involves many steps, it is not possible to explain all the details in a single paper, wherein this paper focuses on presenting the CFM's development and validation, with brief overview on the calibration of essential model parameters and visual examination of simulated profiles of microscopic elements.

The CFM is developed using the modelling concepts provided by GHR type of models. It simulates the microscopic car-following behavior such as dynamic longitudinal interactions between vehicles, and delivers aggregated data of traffic variables to the TC for traffic control purposes. Using the outputs from the CFM, the validation was performed at the macroscopic levels where speed and flow rate for simulated platoons are aggregated in one-minute intervals and are compared with those of field data under various traffic conditions. For simplicity in the model calibration and validation and to capture lane-changing effects, the traffic in the multi-lane expressway where the data were obtained is converted into an equivalent single-lane system.

The CFM model was developed in SIMULINK in MATLAB. It is a graphical programming language that offers modelling, simulation and analyzing of dynamic systems under a Graphical User Interface (GUI) environment [11,20,44]. SIMULINK facilitates easy communication between the simulation with external applications. In SIMULINK the CFM and the TC are harmonized and integrated in a close-loop control system, with the control effects (TC outputs) fed-back as inputs to the CFM in real-time applications.

The structure of the remaining paper is as follows: Section 2 explains the conceptual model, establishes the CFM, and figures out key issues in model's calibration. Section 3 presents the CFM model validation and discusses the model limitations. Section 4 summarizes the research findings and conclusions.

2. Model Development

2.1. Conceptual model

Fig. 1 presents the conceptual model of the TSC for ramp traffic control on expressways. The TSC consists of two main components: car-following model (CFM) and traffic controller (TC). The CFM receives real-time traffic data (flow rate and speed) of the expressway mainline as 'external' inputs, simulates the traffic using car-following behavior and sends aggregated traffic data to the TC, which uses inputs from CFM and 'external' inputs from the MS-FLC such as predicted traffic flows on the expressway mainline to determine the additional ramp flow that can be released to the expressway. Since the control actions implemented by the TC change the traffic condition on the expressway mainline, and this change needs to be captured by the system, the TC's output is fed-back to the CFM. This output is considered the internal input of the CFM, in the sense that both CFM and TC are dependent components of the TSC. For this working mechanism, the TSC functions as a close-loop control system.

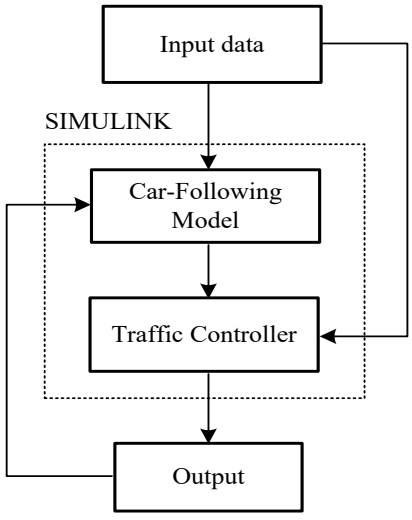

Fig. 1. Conceptual model of the TSC for ramp traffic control on expressways

The TC is the TSC's 2nd component, responsible for implementing the control algorithm as well as calculating traffic parameters for model evaluation. Although the car-following behavior of individual vehicles is simulated, the parameters of interest from the model are the aggregated outputs such as average speed and flow rate.

For evaluation of the MS-FLC a simplified network (Fig. 2) is used. The network has an expressway mainline and a ramp, where the expressway mainline is divided into upstream ramp section and a downstream ramp section. To see the effect of the TSC control in presence of an incident, the downstream ramp section is sub-divided into upstream

incident segment (whose length is denoted as L_{upstr}), and downstream incident segment (whose length is denoted as $L_{downstr}$).

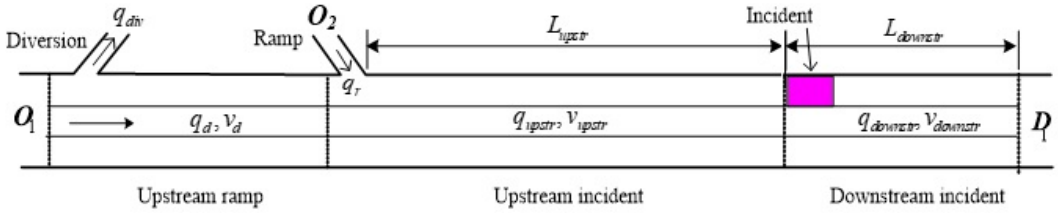

Fig. 2. Layout of the simplified network for MS-FLC evaluation

The overall architecture of the TSC implementation model for the MS-FLC evaluation is presented in Fig. 3. The CFM receives real-time traffic data upstream of the ramp from the "Model Input" to simulate the car-following behavior, then provides the data on vehicle trajectories in the forms of positions and speeds of cars (see also outputs 1 and 2 in the CFM, Fig. 6 below). These CFM's outputs are used to calculate the aggregated data as an internal input of the TC, which uses this internal input at the current time interval, and the predicted traffic flow in the incoming interval to derive the ramp metering flow for the current interval. Given the effect of the control action, the TC calculates the traffic variables, including flow rate, speed, density and travel time for the upstream incident segment (denoted as "Upstr" in Fig. 3), and downstream incident segment (denoted as "Downstr"). Finally, the traffic variables in each time interval are stored in the "Model Output.

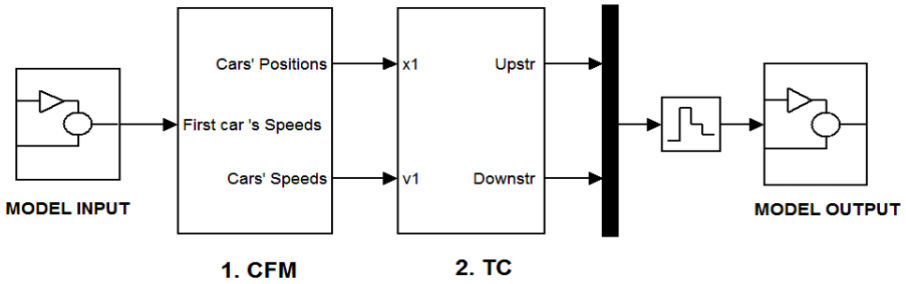

Fig. 3. Overall architecture of the TSC implementation model

Since the CFM is essential in the TSC model, and is presented in this paper, the following section describes the key derivational backgrounds for the CFM development.

2.2. CFM

The CFM developed in this section uses the modelling concepts from Gazis-Herman-Rothery (GHR) family of models in Gazis et al. (1961) [45]. A CFM regulates driver's behavior in relation to the preceding vehicle on the same lane. In the model, the relationship between the leader and the following vehicles is a stimulus-response type, in which the following vehicle's acceleration/deceleration is proportional to its speed, the relative speed, and spacing between the leader and the following vehicles.

The modelling of car-following and traffic-flow behavior necessitates a mathematical representation that captures the most significant aspect of the drivers' behavior [17]. The car-following theory is applied to simulate how vehicles follow each other. Fig. 4 illustrates a two-vehicle system that runs from left to right.

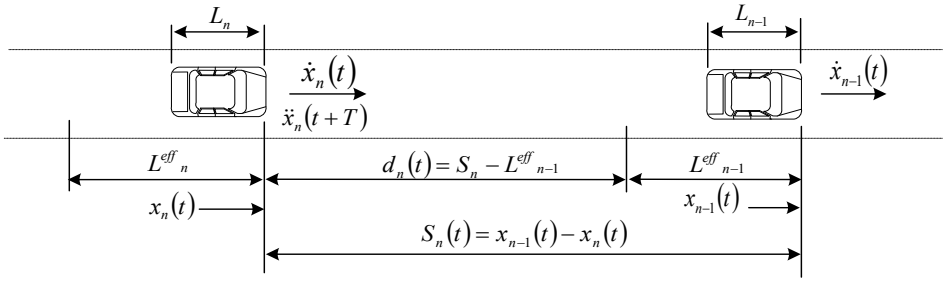

Fig. 4. Car-following diagram

Notations in the car-following theory are defined ad follow:

$n-1$: Lead vehicle

n : Following vehicle

L_{n-1} : Physical length of the lead vehicle

L_n : Physical length of the following vehicle

L_{n-1}^{eff} : Effective length of the lead vehicle, being the sum of the physical length and the minimum distance between stationary vehicles. The distance is defined so as to satisfy performance and/or safety criteria.

L_n^{eff} : Effective length of the following vehicle

$x_{n-1}(t)$: Position of the lead vehicle

$x_n(t)$: Position of the following vehicle

$\dot{x}_{n-1}(t)$: Speed of the lead vehicle

$\dot{x}_n(t)$: Speed of the following vehicle

$\ddot{x}_n(t+T)$: Acceleration rate (deceleration rate) of the following vehicle

T : Reaction time, depending on the driver's characteristics and traffic condition.

Spacing between vehicles:

$$S_n(t) = x_{n-1}(t) - x_n(t) \tag{1}$$

Vehicle following distance:

$$d_n(t) = \left(x_{n-1}(t) - L^{eff}{}_{n-1}\right) - x_n(t) \tag{2}$$

Relative speed:

$$\Delta\dot{x}_n(t) = \dot{x}_{n-1}(t) - \dot{x}_n(t) \tag{3}$$

Time gap:

$$g_n(t) = \frac{x_{n-1}(t) - x_n(t)}{\dot{x}_n(t)} \tag{4}$$

The acceleration (or deceleration) of the following vehicle $\left(\ddot{x}_n\right)$ is considered to occur at time $t+T$. If the relative speed is positive the lead vehicle has a higher speed, then the spacing is increasing. By contrast, if the relative speed is negative the following vehicle has a higher speed, then the spacing is decreasing. Similarly, if the $\ddot{x}_n(t+T)$ value is positive then the following vehicle is accelerating, and if the $\ddot{x}_n(t+T)$ value is negative then the following vehicle is decelerating. Eq. (5) indicates that the acceleration of the following vehicle is a function of the relative movements of the two vehicles, including positions and speeds:

$$\ddot{x}_n(t+T) = f\left(x_{n-1}(t), x_n(t), \dot{x}_{n-1}(t), \dot{x}_n(t)\right) \tag{5}$$

The generic expression of Equation (5) can be represented in a more specific form as Eq. (6)[16]:

$$a_n(t) = c \times v_n^m(t) \times \frac{\Delta v(t-T)}{\Delta x^l(t-T)} \tag{6}$$

where a_n and v_n are respectively the acceleration and speed of n^{th} vehicle at time t; Δx and Δv are respectively the spacing and relative speed between n^{th} and $(n\text{-}1)^{th}$ vehicles at time $t\text{-}T$; T is the reaction time; m, l, and c are the constants to be determined. In the GHR model $m = 1$, $l = 1$, $c = 1$.

Fig. 5 illustrates the key elements of the acceleration (or deceleration) rate. In the *car-following regime*, the acceleration (or deceleration) rate consists of two components:

$$\ddot{x}_n(t+T) = K_1(e_1) \times e_1 + K_g(e_g) \times e_g \tag{7}$$

where $K_1(e_1)$ and $K_g(e_g)$ are the gain parameters, reflecting driver behavior and aggressiveness. Ranges of calibrated values of $K_1(e_1)$ and $K_g(e_g)$ are shown in Table 1; e_1 is the response of the following vehicle to the speed and spacing relative to its front vehicle.

$$e_1 = \frac{\dot{x}_{n-1} - \dot{x}_n}{\left(x_{n-1} - L_{n-1}^{eff}\right) - x_n} \tag{8}$$

If the relative speed is small and the spacing is large the value of e_1 may be negligible and can be discarded, the following vehicle adjusts its acceleration to attain *its desired speed*. This situation correspond to *free-flow regime* the vehicle's speeds are insensitive to the speeds and positions of the vehicles in front. The Equation (7) becomes:

$$\ddot{x}_n(t+T) = K_g(e_g) \times e_g \tag{9}$$

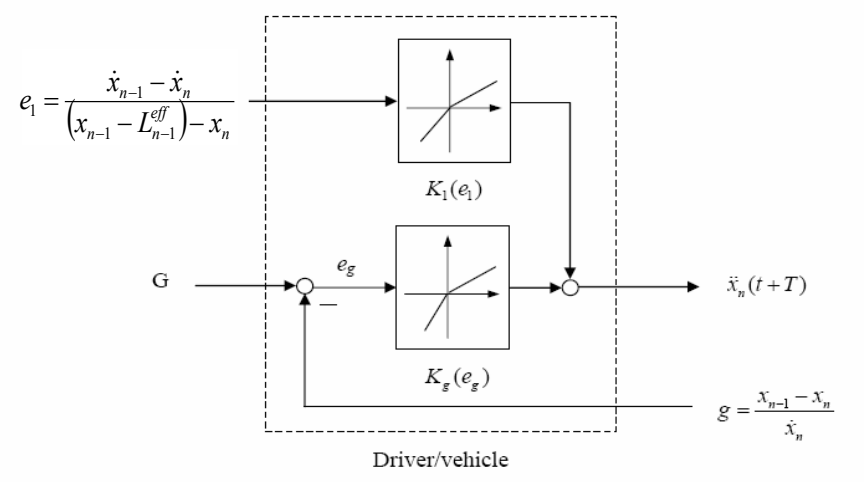

Fig. 5. The block diagram for acceleration/deceleration

The CFM was created in SIMULINK and is presented in Fig. 6. The first vehicle's speed profile is provided, while the time gaps (g) between vehicles at the origin are implicitly provided through flow rates: SIMULINK reads historical database (HDB) from volume and speed reference matrices, provided in 5-minute intervals. Since 5-minute interval is too long for the generation of vehicles, it is divided into shorter intervals (1 second, 5 seconds, or 10 seconds, etc., specified by the user). The generation of the number of vehicles in each short interval considers two cases:

- In *non-congested conditions* the number of the vehicles generated in each short interval (counting distribution) is approximated by Poisson distribution:

$$P_n(t) = \frac{(\chi t)^n}{n!} e^{-\chi t} \tag{10}$$

  where χ denotes the mean rate of the arrivals calculated from the field data in the HDB (in 5-minute interval); t is the time of short interval; n is the number of arrivals in each short interval. In SIMULINK, in the *free-flow regime*, vehicles were generated using the Poisson Integer Generator.
- In *congested conditions*, vehicles are more uniformly distributed along the highway, the mean headways are calculated directly using the flow rates given by the reference volume matrix from the HDB.

The time gaps between vehicles are continually adjusted with changes in the traffic flows. In the network, vehicles' speeds are adjusted according to the time gaps with the vehicles immediately in front. In the CFM the acceleration and speed integrators are used to construct vehicle trajectories, which is progressively updated every 0.1 second during the simulation.

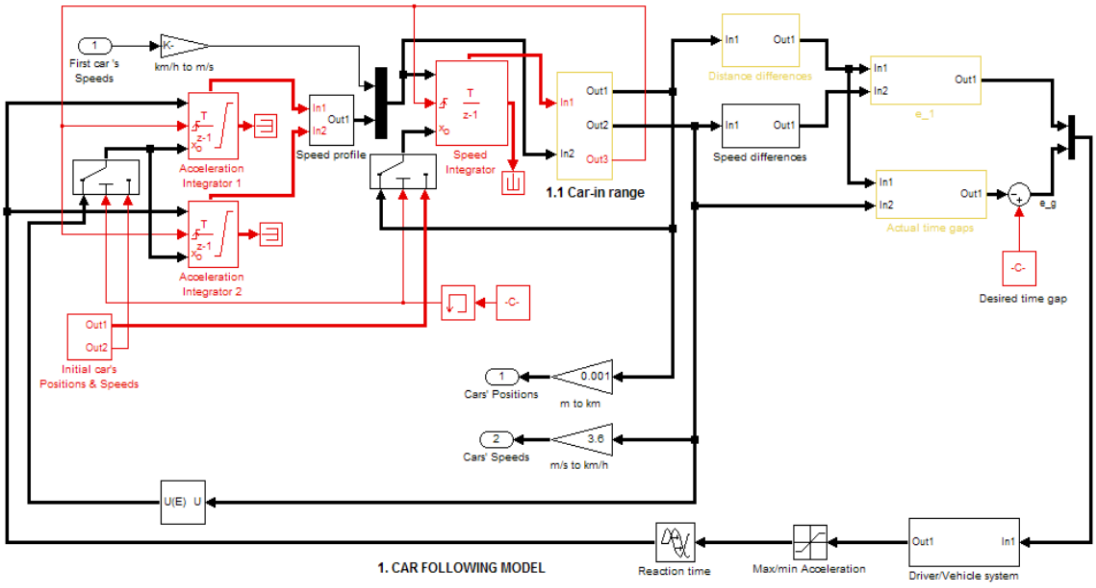

Fig. 6. Car-following model

2.3. Model calibration

By comparing the model to the real system, the CFM calibration aims to identify and tune the parameters that affect model accuracy. The CFM model's kernel is the acceleration/deceleration behavior. In the real world, this behavior is influenced by a variety of factors such as the aggressiveness and awareness of the driver, network geometry, road impediments, vehicle type, and so on, therefore a CFM normally has a significant number of parameters to calibrate. Because the amount of calibration effort grows rapidly as the number of parameters increases, it is preferable to maintain the number of parameters as low as feasible [8,27,41]. The selection of parameters for calibration can be made using engineering judgment.

Given that the CFMs only capture the following driving behavior, the CFM developed in this study implicitly incorporates lane-changing effects through conversion of multi-lane traffic into a single-lane equivalent system using macroscopic variables. There are a number of reasons for CFM calibration at the macroscopic level: (i) the parameters of interest are aggregated data; (ii) in conversion of a multi-lane highway into a single equivalent lane using data aggregated across the lanes the CMF can implicitly capture lane-changing effects by adjustment of its model parameters; (iii) aggregated data are easily obtainable, thus macroscopic calibration avoids the difficulties in collecting observed vehicle trajectories for microscopic calibration.

Since the traffic composition varies between lanes and with time, the equivalent lane flow rate is computed as the weighted average flow rate, and the equivalent lane average speed is computed as the harmonic mean speed across the lanes, taking into account the lateral distribution among lanes in different periods. Details in conversion of a multi-lane into a single lane system are elaborated in Section 3.1, Eq. (11) and Eq. (12). The weighted average flow rate is used to calculate the mean time headway in the CFM, and the computed harmonic mean speed is used as the average speed of individual vehicles. The HDB stores flow rates and speeds in five-minute intervals in the study area (Fig. 7) along the Pan Island Expressway (PIE) of Singapore to calculate the average flow rates and speeds and to learn the speed variances in various traffic conditions. Since five-minute interval is too long for the generation of vehicles, the data were scaled out into one-minute interval for use in the CFM.

In this study, the calibration was conducted at a macroscopic level based on scatter plots of speed–flow diagrams as described in Menneni and Vortisch (2008) [46]. The historical profiles of actual loop detector data (speed and flow rate) on five segments (IDs 80007758, 80007762, 80007766, 80007770, and 80007774) in the study area along the Pan-Island Expressway (PIE) of Singapore (Fig. 7) was used for the model calibration. Since the objective functions does not have closed form [22], the error between simulation and observed data was reduced using a trial-and-error iterative procedure. The CFM parameters were calibrated under free-flow, medium congestion and heavy congestion.

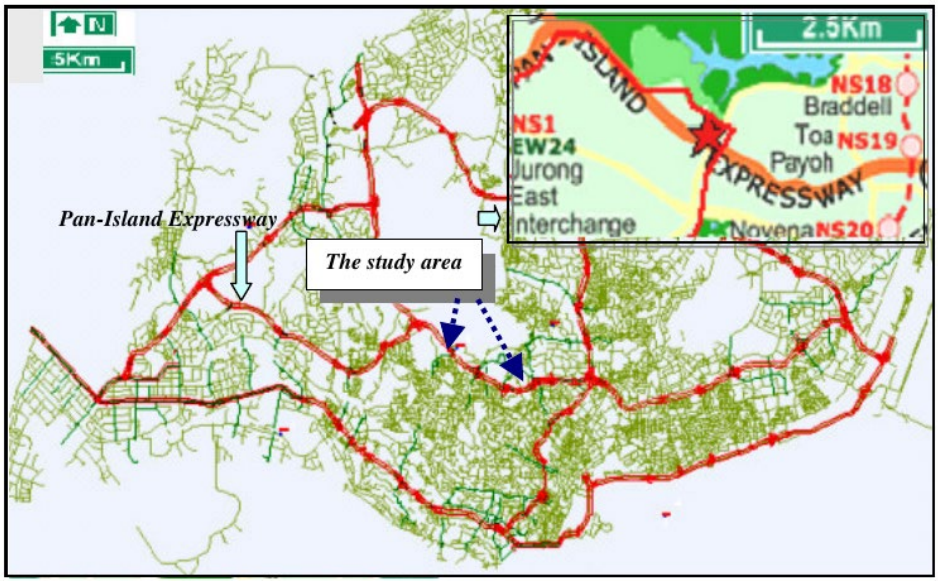

Fig. 7. The study area

Since the MS-FLC uses fuzzy logic concept in the broader research project, this study adopts the fuzzy concept to classify the traffic condition into various congestion levels, including FreeFlow, Light, Medium, Heavy, and VeryHeavy, known as fuzzy predicates. There is no clear-cut but overlaps between the predicates. Fuzzy partitioning of the congestion levels is made with reference to [47] using the level of services (LOS A, B, C, D, E, F) concept introduced in [48]. In this study we considered three congestion levels: free-flow, medium congestion, and heavy congestion. Essentially, FreeFlow is associated with LOS A and partly to LOS B; Medium congestion describes operation primarily at LOS D, partly with LOS C and LOS E, and Heavy congestion primarily describes traffic condition approaching the road capacity (LOS E), and partly to LOS D. Different ranges of model parameters are used to describe different states.

Fig. 8 illustrates the speed-flow relationship for segment 80007762 of the study area using data from the HDB. The figure shows common characteristics of speed-flow relationships in conventional traffic engineering practices.

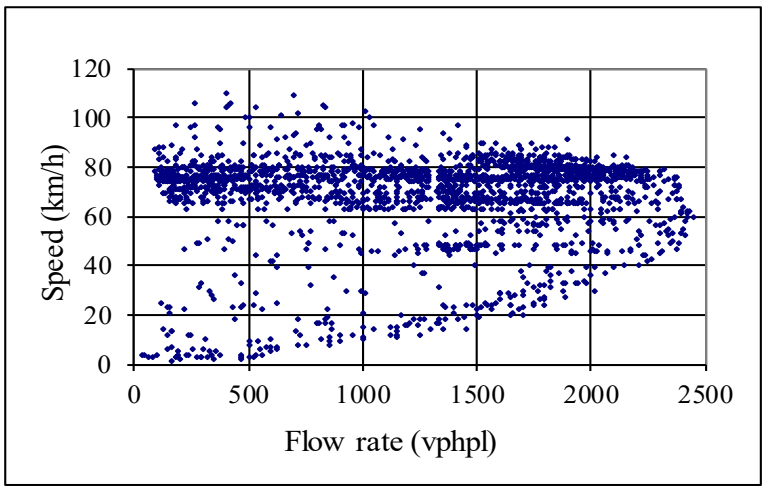

Fig. 8. Speed-volume relationship on segment 80007762

Table 1 summarizes the acceptable ranges of values for the key parameters under various traffic conditions. Since the classification of the traffic congestion level is fuzzy based, the selection of parameters' value also follows the fuzzy based approach, considering two traffic flow regimes: non-congested and congested conditions as stated in Section 2.2. Empirically, each regime covers approximately 60-70% [49] of the "range of values" (Table 1). For example, vehicles in the congested condition have a desired gap (G**) chosen in the lower range [1.25-2.5] (s), and

vehicles in the non-congested condition have a desired gap in the higher range [2.0-3.5] (s). This mean there are no clear cut, but 10-20% overlap between the fuzzy predicates.

Table 1. The most acceptable ranges of parameters in the CFM

(Note: (*): variable. The lower limit corresponds to lower speed, and vice versa; (**): value depends on human factors and traffic condition)

Index	Parameter	Unit	Range of values
1	Desired gap G **	sec.	1.25 to 3.5
2	Gain factor for acceleration $K_{1,a}$ *	m/s	0.7 to 1.0
3	Gain factor for acceleration $K_{g,a}$ *	m/s^3	-1.5 to -1.0
4	Gain factor for deceleration $K_{1,d}$ *	m/s	0.7 to 1.0
5	Gain factor for deceleration $K_{g,d}$ *	m/s^3	-1.2 to -1.0
6	Maximum acceleration a_{max}	m/s^2	3.0
7	Maximum deceleration d_{max}	m/s^2	-3.0
8	Desired speed	km/h	80
9	Reaction time T**	sec.	0.75 to 1.50

The following section presents car-following behavior in a n-vehicle system across a simulated expressway segment with the length of 1.5 km, simulation time of 3,600 seconds, and the desired gap of 3.5 seconds. The model parameters are taken in the range listed in Table 1. The simulated expressway segment is extended before its start point and after its end point by a dummy link whose length is not limited. The vehicles on the dummy link behave similarly to those in the simulated segment. As a result, as soon as the vehicles reach the simulated network, stable conditions can be achieved. When joining the platoon in the dummy link, the last vehicle immediately attains its speed, which is equal to the speed of the vehicle in front.

Fig. 9 shows a zoom of the vehicles' positions and speeds from the simulation profiles for the first two hundred seconds. The trajectory of each vehicle is depicted in Fig. 9 (upper part) by a curve (diagonal) made up of a set of colors, each color representing the vehicle's position in the traffic stream: the first vehicle is represented by the yellow segment, the second vehicle by the magenta segment, and so on. The platoon is headed by a first vehicle at any instance t. When the first vehicle passes the simulated boundary's end to the dummy link, and the following vehicle reaches the end, the first vehicle is disconnected from the system and joins the platoon in the dummy link. The order of the vehicles is also changed at the same time: the second vehicle becomes the first, the third vehicle becomes the second, and so on.

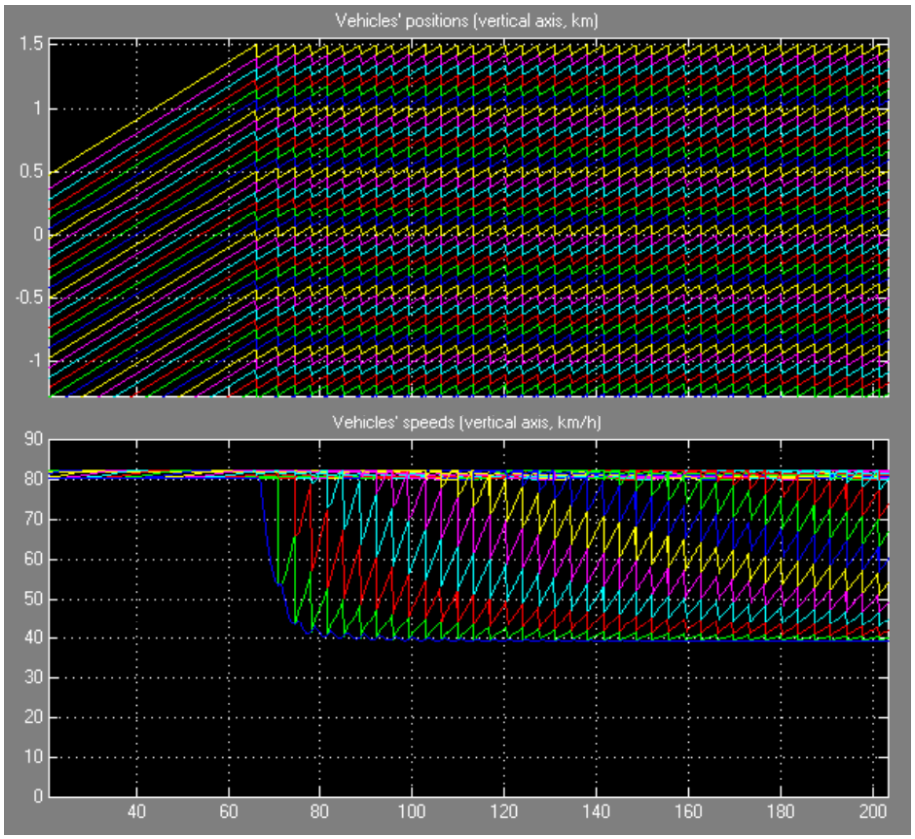

Fig. 9. A zoom in the simulation profiles of vehicles' positions and speeds

The vehicle speeds are depicted in the lower part of Fig. 9. The speeds vary between 40 and 81 km/h. When a vehicle joins the platoon via the dummy link, its speed is set to match the front vehicle's. Following that, the cars' speeds are adjusted to the gaps available: if the gap is larger than the desired gap, the vehicles accelerate; if the gap is smaller, the vehicles decelerate. With the average desired time gap set at 3.5 seconds, for the 200 seconds, the number of vehicles released by the simulation is approximately 60 vehicles, but only more than first half of them were presented in the zoomed in snapshot in the upper part of Fig. 9. Most of the leading vehicles in this platoon attain nearly uniform speed of 80-81km.h, but from the 67 sec.th, due to the increased flow rate, several vehicles in the end of platoon reduce speed gradually (from 80km/h to 41km/h) due to backward-forming shock wave to maintain desirable time gap of 3.5s.

The simulation's vehicle spacing, time gap, and acceleration/deceleration are plotted in Fig. 10. The figure demonstrates that vehicle spacing varies largely between 40 and 80 m, with greater values indicating vehicles in front of the platoon and smaller values indicating vehicles at the rear of the platoon. With the exception of the first 300 seconds, which served as a "warm-up" period, traffic remained stable until the 2,500th second, as seen by relatively constant spacing, time gaps, and low acceleration/deceleration values. The time gaps fluctuated around the desired gap of 3.5 seconds, while the acceleration/deceleration varied between -0.12 and +0.3 m/s2. From the 2,500th second there was a disturbance of traffic condition in the platoons, and the spacing, time gap and acceleration fluctuate more widely: the spacing between vehicles change in the range 30 - 88 m, the time gaps deviated far away from the desired gap, from 2.4 to 4.6 seconds, leading to the change in the acceleration/deceleration, from -2 to +2 m/s2. These ranges reflect realistic behavioral features of traffic in stop-and-go conditions.

The disturbance was made by creating a “planned” fluctuation (down and up) in speed from timestamp 2500th second in SIMULINK. Under a normal situation, the vehicle speeds are approximately equal. At the time 2500th second, the speed of a “leading” vehicle decreased, resulting in a negative relative speed between the “leading” vehicle and the immediately following vehicle. As a result, the following vehicle decelerated with response e_1, as is shown in Eq. (8). This deceleration of the following vehicle automatically causes similar phenomenon the subsequent vehicles in the traffic stream to maintain a desired time gap of 3.5 seconds in the “backward forming shockwave” manner. The propagation speed of the shockwave depends on the “pre-shock” vehicle interaction, i.e density and speed of the traffic stream.

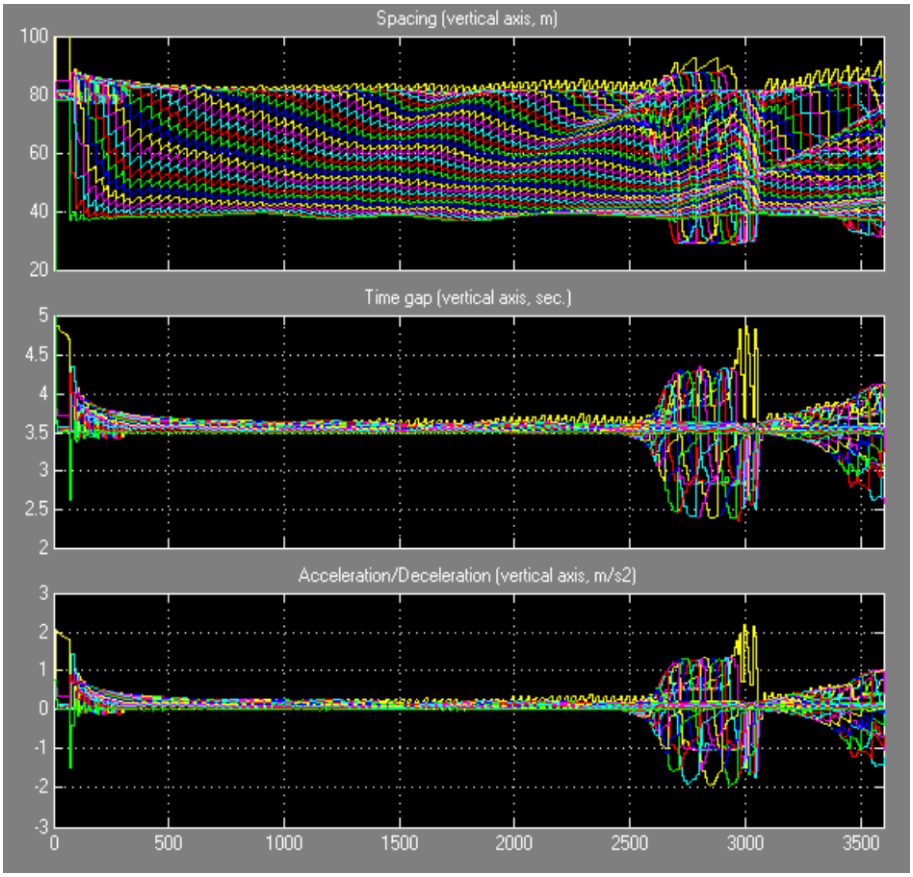

Fig. 10. Vehicle's spacing, time gap, and acceleration (n-vehicle system)

On the contrary, as the speed of the leading vehicle was made increased greater than that of the following vehicle, the relative speed between it and the "leading" vehicle becomes positive, the following vehicle accelerated with response e_1 as the above formulae. This up and down situation occurs with cyclic change in spacing, time gaps, acceleration/deceleration for approximately 10 minutes when the speed of the 1st vehicle was fixed to a constant speed.

3. Model validation

3.1. The site

The expressway portion of the PIE from Mount Pleasant Road to Jalan Toa Payoh was selected for model validation (Fig. 11). There were no impediments (roadwork, traffic accident) or geometric problems on the location. The stretch includes three lanes in each direction, with the upstream link 103066282 of 292 m and the downstream link 103058526 of 337 m in length.

There is an on-ramp from the Mount Pleasant Road. The data used for validation is the historical OD demands in the HDB [50, 51], aggregated in 5-minute intervals. Since the network has only two OD pairs (upstream link - downstream link, and ramp - downstream link, in Fig. 11), the link counts directly reflect the OD demands.

Three typical traffic conditions were selected for the validation: free flow, medium congestion, and heavy congestion during peak, off-peak and night-time periods. There is no control at the ramp. Traffic demand from the ramp ranges between 200 and 800 veh./h, depending on the time of day.

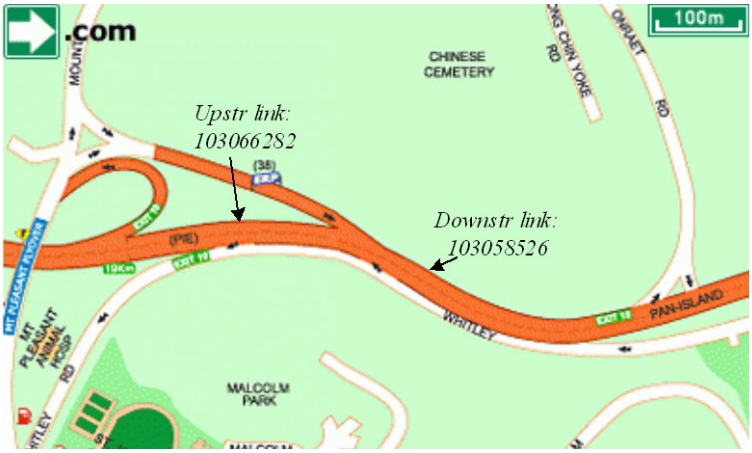

Fig. 11. Actual site for model validation

For simplicity, the traffic in the multi-lane expressway where the data were obtained is represented as an equivalent single-lane system. Since traffic composition varies considerably between lanes and with time of day, the equivalent lane flow is computed as the weighted average flow, while speed is the harmonic mean speed of the three lanes, considering the lateral distribution among lanes in different periods.

$$q_{eq}(t) = \frac{1}{3}\sum_{i=1}^{3}\sum_{j=1}^{N} \xi_j \; p_{ij}(t) q_i(t) \tag{11}$$

where $q_{eq}(t)$ denotes the equivalent lane flow rate in Passenger Car Unit (PCU); ξ_j denotes the Passenger Car Equivalent factor (PCE) of vehicle type *j* converted into PCU; $p_{ij}(t)$ denotes the proportion of vehicle type *j* in lane *i* during interval *t*; $q_i(t)$ denotes the flow rate in lane *i* during interval *t* (veh./h). *N* denotes the number of vehicle types in the traffic stream.

Similarly, the equivalent lane speed $v_{eq}(t)$ is computed as:

$$v_{eq}(t) = \frac{\sum_i v_i(t) \times q_i(t)}{\sum_i q_i(t)} \tag{12}$$

where $v_i(t)$ and $q_i(t)$ are speed and flow rate of lane *i* during interval *t*, respectively. This assumes that platoons of vehicles in each lane travel with the same speeds in each time interval.

The values of ξ_j for the Pan Island Expressway (PIE) in Singapore was proposed with referencing to Fan [51], Fan et al. [52], Yeung et al. [7], and UK Department of the Environment [53]. Among which, the references [7, 51, 52] are for PCE values on Singapore expressways. PCE factors in the UK [53] are included for reference because traffic in Singapore closely resembles that in the UK (left-hand driving, terrain condition). The values were estimated for capacity flow conditions (heavy congestion) for level terrain that is prevailing in Singapore expressways. Under free-flow conditions, it can be expected that heavy vehicles would have a lower effect than under congested conditions [54] since the interaction between heavy vehicles and smaller vehicles is less intense, resulting in more passing opportunities for the smaller vehicles to maintain their desired speeds. The proposed PCE values are shown in Table 2. Given that the references for PCE values under free-flow and medium condition are not available, and the fact that terrain is among the most influencing factors, we propose to use the PCE values in Table 2 as a rough estimate for free-flow and medium condition.

Table 2. PCE equivalent factors for Singapore expressways for capacity flow conditions

Vehicle type (j)	ξ_j
Cars and taxis	1.00
Light goods vehicles	1.30
Heavy trucks	2.60
Buses	2.70
Motorcycles	0.49

The proportion of vehicles $p_{ij}(t)$ is not only lane-specific but also time-dependent. The fastest lane has a higher proportion of cars and vans, whereas the slow lane has a higher proportion of heavy freight vehicles. Temporarily, commuter vehicles may represent the majority of traffic during peak hours, while trucks make up a considerable amount of traffic during off-peak and nighttime periods.

Because collecting data for each segment and time interval is time consuming and costly, it would be reasonable to perform sampling surveys at representative locations during typical time periods, such as peak, off-peak, and midnight. The video-based surveys were carried out on PIE segment 80007770, which has similar physical parameters (lane width, number of lanes) to the simulated location (segment 80007774). The traffic composition and lane distributions may be similar since they are two consecutive segments. The survey times spanned from 45 minutes (AM peak) to 75 minutes (off peak), and all free-flow, medium-flow, and congested conditions were experienced. The results of the data analysis are shown in Table 3, which summarizes the lower bound and upper bound for lateral distributions (number of vehicles on different lanes) under different traffic conditions during various survey periods.

Table 3. Lateral distributions of traffic on PIE

Traffic lane	Lower value (%)	Upper value (%)
Lane 1	39.47	42.10
Lane 2	31.60	35.94
Lane 3	24.62	26.30

The traffic composition was also obtained from the same survey. Table 4 shows the lower and upper values in counting the number of vehicles across the lanes for various types for different 15-minute intervals during AM peaks. In free-flow situations, flow rates may be biased towards the fastest lane (lane 1), whereas in congested situations, traffic tends to spread more evenly throughout lanes. As a result, the use of either extreme values or the average in determining traffic composition is dependent on traffic conditions. The values were used to calibrate parameters in the CFM and to convert the $q_{eq}(t)$ in PCU values in the simulation.

Table 4. Traffic composition on PIE in AM peaks

Vehicle type	Lower value (%)	Upper value (%)
Car	62.60	66.10
Van	6.22	7.55
Light truck	13.70	17.80
Heavy truck	3.20	7.32
Bus	0.50	1.52
Motorcycle	5.23	5.89

The simulated traffic speed and flow rate were compared to the observed data for the upstream and downstream links separately:

- Comparison of simulated counts with actual counts
- Comparison of simulated speeds with actual speeds

The settings of simulation for validation include simulation time of 90 minutes, of which the first 30 minutes being the warm-up period. The parameters of interest are minute-by-minute aggregated speeds and densities, collected from the 31st to 90th minute.

3.2. Model validation

For macroscopic validation, the overall performances of the model are examined instead of comparing the performance of individual vehicles. The macroscopic level validation may not offer as much detailed information about the model capabilities as the microscopic level, because the variables are the average values for all vehicles in the platoon. For instance, while the average speeds for a simulated and an actual platoon might be similar, the speeds of individual vehicles may differ [31]. However, for traffic control we are interested to aggregated data rather than the trajectories of individual vehicles. At the macroscopic level, the average speed and volume for simulated platoons are compared with those of field data. In the following section, the speed is evaluated using statistical hypothesis test (the paired T-test), and the flow rate is evaluated using the Mean Absolute Percentage of Error as a goodness-of-fit measure of performance.

3.2.1. Speed

Since the actual and simulated speeds are collected in pairs, where each pair represents one-to-one correspondence, the paired t-test is used for analyzing the differences between readings of speeds on each interval. Let $(X_{11}, X_{21}), (X_{12}, X_{22}), ..., (X_{1n}, X_{2n})$ be a set of n paired observations where the mean and variance of the population represented by X_1 are μ_1 and σ_1^2, and the mean and variance of the population represented by X_2 are μ_2 and σ_2^2. Define the differences between each pair of observations as $D_j = X_{1j} - X_{2j}, j = 1, 2, ..., n.$ The differences are assumed normally distributed with mean:

$$\mu_D = E(X_1 - X_2) = E(X_1) - E(X_2) = \mu_1 - \mu_2 \tag{13}$$

and variance σ_D^2. The test statistic is:

$$T_0 = \frac{\overline{D} - \Delta_0}{S_D / \sqrt{n}} \tag{14}$$

where $\overline{D}$ is the sample average of the n differences; $D_1, D_2, ..., D_n$, and S_D is the sample standard deviation of these differences.

Table 5 summarizes the actual and simulated speeds (km/h) for upstream segment of the simulation under free-flow condition in the evaluation period, from the 31st to 90th minute, excluding 30 minutes of the warm-up period. The data are aggregated in one-minute interval.

Table 5. Actual and simulated speeds (km/h) on upstream segment

Minute	Actual speed	Simulated speed	Difference	Minute	Actual speed	Simulated speed	Difference
31	71.76	74.43	-2.67	61	83.58	83.37	0.21
32	72.13	75.92	-3.79	62	86.38	86.4	-0.02
33	74.19	76.39	-2.20	63	85.30	88.32	-3.02
34	76.38	78.37	-1.99	64	86.17	86.36	-0.19
35	78.98	76.47	2.51	65	83.05	82.50	0.55
36	80.81	79.52	1.29	66	81.44	83.80	-2.36
37	79.37	81.77	-2.40	67	80.30	81.93	-1.63
38	81.73	83.86	-2.13	68	80.29	79.45	0.84
39	78.91	82.83	-3.92	69	79.20	81.70	-2.50
40	82.29	84.42	-2.13	70	80.59	79.06	1.53

41	80.85	82.29	-1.44	71	80.89	79.47	1.42
42	79.26	80.48	-1.22	72	79.81	78.17	1.64
43	78.73	77.15	1.58	73	82.67	77.37	5.30
44	80.59	81.80	-1.21	74	81.53	83.12	-1.59
45	82.95	81.73	1.22	75	81.41	80.78	0.63
46	85.21	84.29	0.92	76	82.17	79.35	2.82
47	85.69	81.88	3.81	77	81.63	80.24	1.39
48	84.43	81.21	3.22	78	83.42	83.82	-0.40
49	85.79	79.12	6.67	79	83.33	83.79	-0.46
50	83.15	80.29	2.86	80	81.89	82.03	-0.14
51	83.44	81.34	2.10	81	81.36	82.05	-0.69
52	82.97	83.19	-0.22	82	81.44	81.61	-0.17
53	81.88	81.58	0.30	83	79.92	79.42	0.50
54	82.88	80.30	2.58	84	81.89	84.56	-2.67
55	79.8	82.59	-2.79	85	79.44	79.47	-0.03
56	76.73	77.83	-1.10	86	77.55	81.28	-3.73
57	74.22	74.33	-0.11	87	76.35	80.41	-4.06
58	74.15	76.09	-1.94	88	74.99	76.87	-1.88
59	77.12	74.24	2.88	89	73.85	74.81	-0.96
60	81.03	78.36	2.67	90	73.74	74.03	-0.29

The paired t-test for this condition is conducted through the 8-step procedure as follow:

a) The parameter of interest is the difference in the means of actual and simulated speeds, μ_D.
Assume $\mu_D = 0$.

b) Null hypothesis $H_0 : \mu_D = 0$

c) Alternative hypothesis $H_1 : \mu_D \neq 0$

d) Significance level $\alpha = 0.05$

e) The test statistic is:

$$t_0 = \frac{\overline{d}}{s_D / \sqrt{n}} \tag{15}$$

f) Reject H_0 if $t_0 > t_{\alpha/2, n-1} = t_{0.025,\,59} \approx 2$ or if $t_0 < t_{0.025,59} \approx -2.$

g) Calculation: the sample mean and the standard deviation of the differences are $\overline{d} = -0.114$, and $s_D = 2.268$. The resulting test statistic $t_0 = -0.387$

h) Conclusion: Since $t_0 = -0.387 > -2$, the null hypothesis $\mu_D = 0$ cannot be rejected at the significance level $\alpha = 0.05.$

Table 6 summarizes the results from the paired t-test for the upstream and downstream segments under free-low, medium congestion, and heavy congestion. The table shows that the simulated speed is not significantly different from the actual speed at the significance level $\alpha = 0.05$ for both segments under prevailing traffic conditions.

Table 6. Summary of paired t-test for speed analysis

Simulated regime	Segment	$\overline{d}$	S_D	n	t_0	Conclusion
Free flow	Upstream	-0.114	2.268	60	-0.387	Not significantly different
	Downstream	-0.122	2.389	60	-0.396	Not significantly different
Medium congestion	Upstream	0.160	2.599	60	0.470	Not significantly different
	Downstream	-0.114	1.717	60	-0.517	Not significantly different
Heavy congestion	Upstream	-0.242	1.120	60	-1.674	Not significantly different
	Downstream	0.321	1.452	60	1.712	Not significantly different

3.2.2. Flow rate

The accumulated simulated counts are plotted against the actual counts for upstream and downstream links in Figs. 10 to 12 under free-flow, medium congestion, and heavy congestion, respectively. The Figs. show that although the simulated data are slightly undercounted under the medium and heavy congestion, the data pairs stick relatively closely to the perfect lines, represented by diagonals.

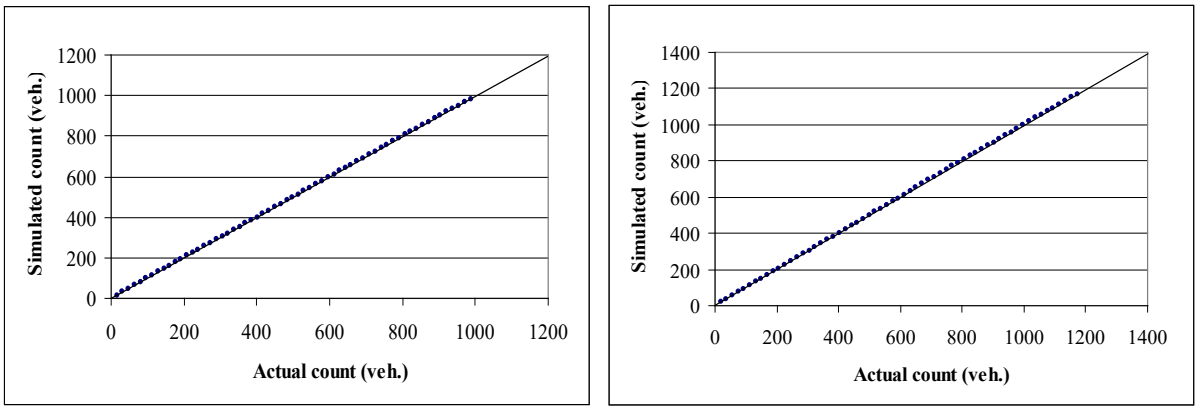

a) Upstream link b) Downstream link

Fig. 12. Simulated versus observed count under free-flow condition

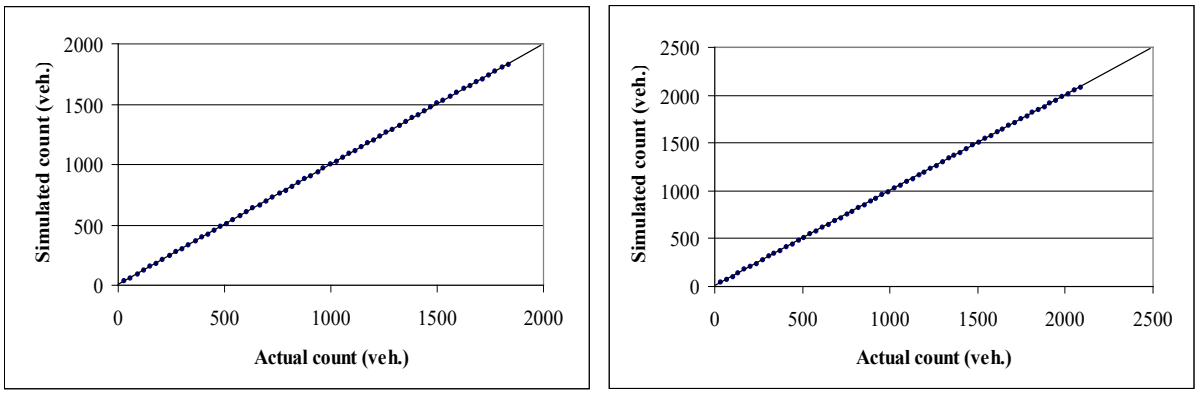

a) Upstream link b) Downstream link

Fig. 13. Simulated versus observed count under medium congestion

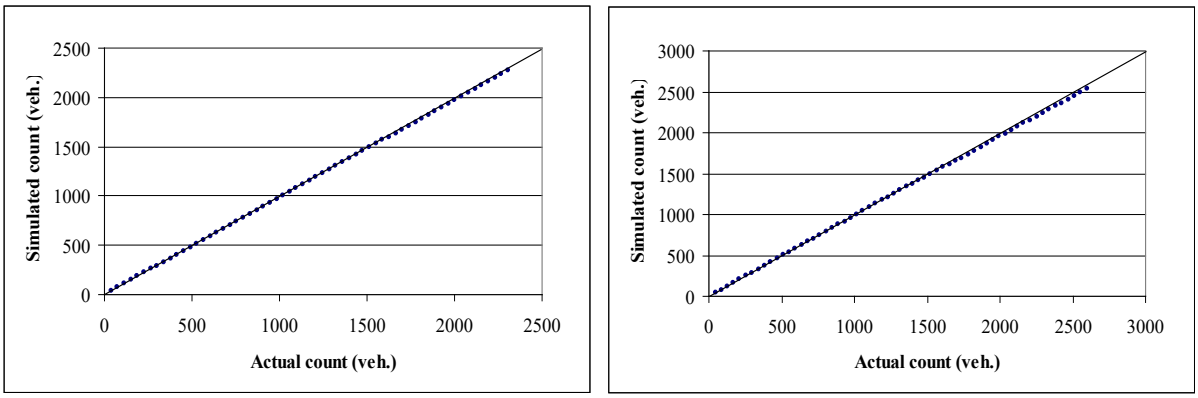

a) Upstream link b) Downstream link

Fig. 14. Simulated versus observed count under heavy congestion

Since the magnitude of absolute errors for traffic volume is large, it may be difficult to envisage using RMSE. Therefore, the Mean Absolute Percentage of Error (MAPE) is used instead:

$$MAPE(\%) = \frac{\sum_{i=1}^{N}\left(\frac{|V_i^a - V_i^s|}{V_i^a}\right)}{N} \times 100 \tag{16}$$

where V_i^a and V_i^s denote the actual and simulated flow rates, respectively, in interval *i; N* is the number of intervals ($N = 60$).

Table 7 lists the MAPEs for simulated traffic counts where the errors vary from 2.21% to 3.15%. Given that the PCE values of heavy vehicles applicable to heavy congestion were used for free-flow and medium congestion, to see the how the change in PCE values affects the prediction errors, we further manipulate the Eq. (16) into Eq. (17).

$$MAPE(\%) = \frac{\sum_{i=1}^{N}\left(\frac{|V_i^a - V_i^s|}{V_i^a}\right)}{N} \times 100 = \frac{\sum_{i=1}^{N}\left(\left|1 - \frac{V_i^s}{V_i^a}\right|\right)}{N} \times 100 \tag{17}$$

Eq. (17) shows that the prediction error (MAPE) is a function of the $\frac{V_i^s}{V_i^a}$ ratio, while the change in PCE values of heavy vehicles affects both quantities V_i^s and V_i^a in the same manner (increase or decrease simultaneously). In other words, it is unlikely that the use of PCE factors of heavy vehicles under congested conditions for free-flow and medium congestion cause a significant error.

Table 7. Errors of simulated flow rates (MAPE, %)

Simulated regime	Upstream link	Downstream link
Free flow	2.21	2.30
Medium congestion	2.54	2.85
Heavy congestion	2.85	3.15

An inspection of results from the simulation shows that the simulated volume has bigger local variations than the actual volume. Fig. 15 shows an example of the absolute percentage of errors from all intervals for the upstream segment, under heavy congestion scenario. Fig. 15 shows that although the MAPE for this scenario is 2.85%, errors of greater than 5% may be noticed in 8 out of 60 intervals.

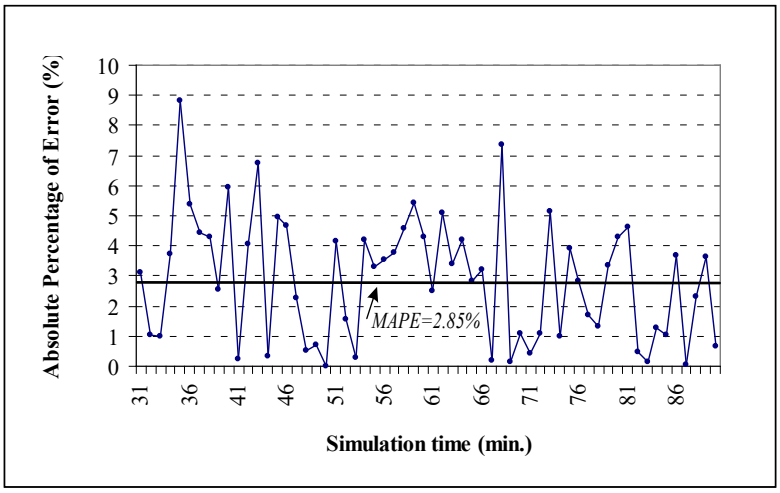

Fig. 15. Absolute percentage of errors on upstream segment *(Heavy congestion)*

3.3. Discussions

The CFM simulates the car-following behavior and delivers the aggregated traffic parameters to the TC for traffic control. In a multi-lane highway, a standard microscopic traffic simulation package incorporates both car-following and lane-changing behavior. The CFM, which is embedded in SIMULINK, replicates car-following behavior in which traffic is transformed to a single-lane equivalent, eliminating the need for lane-changing behavior. Although there are few lane-changing opportunities under crowded conditions, lane-changing maneuvers in free-flowing traffic can have a significant impact on vehicle speeds and travel times. The parameters of interest, on the other hand, are the general macroscopic traffic characteristics that are averaged across lanes and so may not be very sensitive to vehicles' lane changing behavior. As a result, by adjusting its settings, the CFM established in this study indirectly integrates lane-changing effects. An iterative calibration process refines the model's parameters at the same time, ensuring that the model accurately replicates real-world behavior.

Limitation of the CFM

The CFM's development based on the GHR paradigm has several shortcomings. The GHR models presume that the following vehicle reacts to slight changes in relative speed and to the actions of its leader, including large distances. Only when the relative speed is zero does the reaction diminish (see the formulas for the response e_1 in Fig. 5). This may not be properly reflected in actual driver behavior. Psycho-physical models in Brackstone and McDonald (1998) [16] address the issue by using thresholds: drivers react to changes in relative speed or spacing only when these thresholds are reached [55].

Another flaw in the CFM is that it assumes a constant value of reaction time for all vehicles in each traffic scenario, implying that drivers are more attentive in congested traffic and hence have a shorter reaction time than in non-congested situations. This may be true for models used to estimate macroscopic parameters (such as those employed in this study), but it isn't very realistic from a micro perspective because reaction time differs between drivers. One solution to enhance this is to assign reaction times to individual drivers based on a distribution of reaction times derived through detailed field study.

4. Conclusions

This study constitutes part of a broader research project [43] involving the development of a multi-stage fuzzy logic controller (MS-FLC) for ramp traffic control on expressways. The formulation and implementation of actions for ramp control using fuzzy-logic control algorithm is the core of the 3rd stage in the MS-FLC. For these tasks, a traffic simulator and control (TSC) that consists of a driving simulator, named in this paper as the car-following model (CFM), and a traffic controller (TC) was developed. Given that the discussion of the details would be lengthy and exceed the normal range of a typical paper, this paper focuses on presenting the development and validation of the

CFM, with a brief overview of the calibration of essential model parameters and visual examination of simulated profiles of microscopic elements.

The development of the CFM is based on the modeling concepts used in the GHR family of models, in which the relationship between the leader and the following vehicles is modeled as a stimulus-response function, with the following vehicle's acceleration/deceleration proportional to its speed, relative speed, and distance between the leader and the following vehicles. Although individual car-following behaviors are simulated, the aggregated outputs from the model, such as average speed and flow rate, are the parameters of interest.

The validation of the CFM is by comparing its outputs to field data obtained from a stretch of Pan-Island Expressway (PIE) of Singapore. The speed is analyzed using the statistical hypothesis test, whereas the flow rate is evaluated using the MAPE as the goodness-of-fit measure. The results reveal that for both upstream and downstream segments, the simulated speed is not significantly different from the actual speed at the 5% significance level, and the aggregated flow rate disparities are small. This demonstrates that the TSC model is a sound model for traffic simulation and control.

Over the last sixty years, the study of car-following behaviors has progressed from conceptual models to mathematical formulation, model development, and model revision based on empirical testing and evaluation. There have been numerous car-following models built, and they are helpful tools for studying traffic systems and evaluating traffic management and control strategies. This study aims to make a minor contribution to the literature in the field of car-following modeling. The models aim to describe the behavior of macroscopic systems on a bigger scale by analyzing microscopic elements. Future works may be extended to carry out a sensitivity analysis of the model parameters to identify the most critical model parameters, and the recommended range of the parameters associating with various traffic conditions for the model users.

Declaration of competing interest

The authors declare that they have no known competing financial interests or personal relationships that could have appeared to influence the work reported in this paper.

Acknowledgments

The authors highly appreciate the Land Transport Authority (LTA) of Singapore for providing the field data used in this research.

References

[1]. D. Gaye, R.M. Faye, B. Mampassi, A car following model for traffic flow simulation, 9 (2016) 1–9.
[2]. H. Rakha, B. Hellinga, M. Van Aerde, W. Perez, Systematic verification, validation and calibration of traffic simulation models, Proceeding 75th Annu. Meet. Transp. Res. Board. (1996).
[3]. T.V. Mathew, K.K.V. Rao, Microscopic traffic flow modeling, Introd. to Traffic Eng. (2007) 1–9. http://nptel.ac.in/courses/105101087/downloads/Lec-34.pdf.
[4]. D. Ni, J.D. Leonard, A. Guin, B.M. Williams, Systematic approach for validating traffic simulation models, Transp. Res. Rec. (2004) 20–31. https://doi.org/10.3141/1876-03.
[5]. M. Fellendorf, P. Vortisch, Validation of the microscopic traffic flow model VISSIM in different real-world situations, Transp. Res. Board 80th Annu. Meet. (2001) 1–9. http://trid.trb.org/view.aspx?id=689890.
[6]. R. Rebba, S. Huang, Y. Liu, S. Mahadevan, Statistical validation of simulation models, Int. J. Mater. Prod. Technol. 25 (2006) 164–181. https://doi.org/10.1504/ijmpt.2006.008280.
[7]. J.S. Yeung, Y. D. Wong, J. R. Secadiningrat, Lane-harmonized passenger car equivalents for heterogeneous expressway traffic, Transportation Research Part A 78 (2015) 361–370).
[8]. P. Maheshwary, K. Bhattacharyya, B. Maitra, M. Boltze, A methodology for calibration of traffic micro-simulator for urban heterogeneous traffic operations, J. Traffic Transp. Eng. (English Ed. 7 (2020) 507–519. https://doi.org/10.1016/j.jtte.2018.06.007.
[9]. D.C. Gazis, R. Herman, R.B. Potts, Car-following theory of steady-state traffic flow, Oper. Res. 7 (1959) 499–505. https://doi.org/10.1287/opre.7.4.499.
[10]. A.D. May, Introduction to traffic flow theory, 1997. https://doi.org/10.1016/b978-034066279-3/50018-9.
[11]. S.A. Boxill, L. Yu, An evaluation of traffic simulation models for supporting ITS development, (2000).

[12]. R. Dowling, A. Skabardonis, J. Halkias, G. McHale, G. Zammit, Guidelines for calibration of microsimulation models: Framework and applications, Transp. Res. Rec. (2004) 1–9. https://doi.org/10.3141/1876-01.
[13]. A. Sharma, Understanding and modelling the car-following behaviour of connected vehicles, (2019).
[14]. K. Fadhloun, H. Rakha, A. Loulizi, J. Wang, A validation study of the fadhloun-rakha car-following model, VEHITS 2020 - Proc. 6th Int. Conf. Veh. Technol. Intell. Transp. Syst. (2020) 180–192. https://doi.org/10.5220/0009435501800192.
[15]. M. Errampalli, S.S. Mallela, S. Chandra, Calibration of car-following model for Indian traffic conditions, Transp. Res. Procedia. 48 (2020) 829–839. https://doi.org/10.1016/j.trpro.2020.08.091.
[16]. M. Brackstone, M. McDonald, Car-following: a historical review. Transportation Research Part F: Traffic Psychology and Behavior, Vol. 2, No. 4, pp. 181-196, 1999.
[17]. H. Rakha, Y. Gao, Calibration of steady-state car-following models using macroscopic loop detector data, Final Rep. VT-2008-01 (2010) 24.
[18]. M. Rahman, Application of parameter estimation and calibration method for car-following models, (2013), All Theses. 1763, https://tigerprints.clemson.edu/all_theses/1763.
[19]. S. An, L. Xu, L. Qian, G. Chen, H. Luo, F. Li, Car-following model for autonomous vehicles and mixed traffic flow analysis based on discrete following interval, Phys. A Stat. Mech. Its Appl. 560 (2020). https://doi.org/10.1016/j.physa.2020.125246.
[20]. V.S.P. Pasumarthy, Formulations, issues, and comparison of car-following models, Master thesis, Virginia State University (2004).
[21]. R. Liu, J. Wang, A general framework for the calibration and validation of car- following models along an uninterupted open highway, Transport. (2007) 1–13.
[22]. V. Kanagaraj, G. Asaithambi, C.H.N. Kumar, K.K. Srinivasan, R. Sivanandan, Evaluation of different vehicle following models under mixed traffic conditions, Procedia - Soc. Behav. Sci. 104 (2013) 390–401. https://doi.org/10.1016/j.sbspro.2013.11.132.
[23]. P.G. Gipps, A behavioral car-following model for computer simulation. Transp. Res. B, 15 (1981) 105-111.
[24]. W. Leutzbach, R. Wiedemann, Development and applications of traffic simulation models at the Karlsruhe Institut Fur Verkehrwesen, TE&C 27 (1986), 270-278.
[25]. H.M. Zhang, T. Kim, A Car-following theory for multiphase vehicular traffic flow. 80th TRB Annual Conference, Washington D.C (2001).
[26]. S. Panwai, H. Dia, Comparative evaluation of microscopic car-following behavior, IEEE Transactions on Intelligent Transportation Systems, 6(3) (2005) 314-325.
[27]. J.J. Olstam, A.Tapani, Comparison of car-following models. VTI meddelande 960A, Swedish National Road Administration (2004).
[28]. D. Chen, Y. Yuan, B. Li, J. Wu, Validation and comparison of microscopic car-following models using beijing traffic flow data, Lect. Notes Comput. Sci. 3614 LNAI (2006) 1008–1011.
[29]. X. Li, X. Luo, M. He, S. Chen, An improved car-following model considering the influence of space gap to the response, Phys. A Stat. Mech. Its Appl. 509 (2018) 536–545. https://doi.org/10.1016/j.physa.2018.06.069.
[30]. B.R. Hellinga, Requirements for the calibration of traffic simulation models, Proc. Canada Soc. Civ. Eng. 1998 Anuual Conf. Held Halifax. IVB (1998) 1689–1699.
[31]. R.F. Benekohal, Procedure for validation of microscopic traffic flow simulation models, Transp. Res. Rec. (1991) 190–202.
[32]. M. Ben-Akiva, D. Cuneo, M. Hasan, M. Jha, Q. Yang, Evaluation of freeway control using a microscopic simulation laboratory", Transportation Research Part C 11 (2003) 29-50.
[33]. L. Rao, L. Owen, D. Goldsman, Development and application of a validation framework for traffic simulation models, Winter Simul. Conf. Proc. 2 (1998) 1079–1086. https://doi.org/10.1109/wsc.1998.745856.
[34]. Y. Zhang, L.E. Owen, Systematic validation of a microscopic traffic simulation program, Transp. Res. Rec. (2004) 112–120. https://doi.org/10.3141/1876-12.
[35]. J.F. Torres, A. Halati, A. Gafarian, Statistical guidelines for simulation experiments, executive summary, JFT Associates, Culver City (1983).
[36]. A.V. Gafarian and J.D. Walsh, Methods for statistical validation of a simulation model for freeway traffic near an onramp, Transportation Research 4 (1970) 379- 324.
[37]. M. Treiber, A. Kesting, Microscopic calibration and validation of car-following models – a systematic approach, Procedia - Soc. Behav. Sci. 80 (2013) 922–939. https://doi.org/10.1016/j.sbspro.2013.05.050.
[38]. Y. Wang, M. Papageorgiou, A. Messmer, Real-time freeway traffic state estimation based on extended kalman filter: Adaptive capabilities and field data testing, Transportation Research Part A: Policy and Practice 42 (10) (2008) 1340–1358.
[39]. E. Jenelius, I. Kristoffersson, M. Fransson, Validation of traffic simulation models based on the macroscopic fundamental diagram, Transp. Res. Procedia 27 (2017) 561–568. https://doi.org/10.1016/j.trpro.2017.12.073.
[40]. R.F. Benekohal, J. Treiterer, CARSIM. Car-following model for simulation of traffic in normal and stop-and-go conditions, Transp. Res. Rec. 2 (1988) 99–111.
[41]. B.N. Matcha, S.N. Namasivayam, M. Hosseini Fouladi, K.C. Ng, S. Sivanesan, S.Y. Eh Noum, Simulation strategies for mixed traffic conditions: a review of car-following models and simulation frameworks, J. Eng. (United Kingdom).

2020 (2020). https://doi.org/10.1155/2020/8231930.
[42]. M. Brackstone, M. Montanino, W. Daamen, C. Buisson, V. Punzo, Use, calibration, and validation of traffic simulation models in practice: results of web-based survey. TRB 2012 - Transportation Research Board 91rd Annual Meeting, Jan 2012, Washington D.C, United States. 12 p. hal-01411970.
[43]. T.D. Toan, M. Meng, S.H. Lam, Y.D. Wong, Multi-stage fuzzy logic controller for expressway traffic control during incidents, Fortcoming paper, to apprear in Journal of Transportation Engineering, Part A: Systems, March (2022).
[44]. MATLAB. User Manual, Version 6.5, Release 13 (2002).
[45]. D.C. Gazis, R. Herman, R. Rothery, Non-linear follow-the-leader models of traffic flow, Operations Research 19 (1961) 545-567.
[46]. S. Menneni, C. Sun, P. Vortisch, Microsimulation calibration using speed-flow relationships. Transportation research board 2088, Washington (2008) 1–9.
[47]. J.G. Nicholas, L.A. Hoel, Traffic and Highway Engineering, fourth ed., University of Virginia, 2009.
[48]. Highway Capacity Manual, Transport Research Board, National Research Council, Washington, D.C., 2000.
[49]. T.D. Toan, Development of a fuzzy knowledge-based system for local traffic control for incident management, PhD Thesis, School of Civil & Environmental Engineering, Nanyang Technological University (2008).
[50]. T.D. Toan, Y.D. Wong, Fuzzy logic-based methodology for quantification of traffic congestion, Physica A: Statis. Mec. and its App. 570, (2021) 125784.
[51]. H.S.L. Fan, Passenger car equivalents for vehicles on Singapore expressways, Transportation Research A, 24(3) (1990) 391-396.
[52]. H.S.L. Fan, C.L. Mak, Y. D. Wong, Passenger car units of vehicles on Singapore roads Centre for Transportation Studies, Singapore (1997).
[53]. UK Department of the Environment, Roads in Urban Areas. HMSO, London (1966).
[54]. A. Al-Kaisy, Y. Jung, H. Rakha, Developing passenger car equivalency factors for heavy vehicles during congestion, Journal of Transportation Engineering ASCE, 131(7) (2005) 514-523.
[55]. W. Leutzbach, Introduction to the theory of traffic flow. Berlin, Springer Verlag (1988).